Modelling precipitation of niobium carbide in austenite: multicomponent diffusion, capillarity, and coarsening

N. Fujita and H. K. D. H. Bhadeshia

The growth of niobium carbide in austenite involves the diffusion of both niobium and carbon. These elements diffuse at very different rates. A model is presented for the overall transformation kinetics of niobium carbide precipitation in austenite that takes into account the multicomponent nature of the diffusion process while at the same time allows for the curvature of the transformation front. The inclusion of the curvature (capillarity) effect has, in a numerical scheme, permitted the precipitation and coarsening reactions to be treated in a single model. The model is compared with published experimental data. **MST/4716**

The authors are in the Department of Materials Science and Metallurgy, University of Cambridge, Pembroke Street, Cambridge CB2 3QZ, UK. *Manuscript received 5 June 2000; accepted 12 September 2000.*

Introduction

Niobium is a strong carbide forming element which is used widely in microalloyed steels to control the austenite grain size during the thermomechanical processing of vast quantities of structural steels.[1–4] Naturally, its formation involves the diffusion of both substitutional niobium and interstitial carbon. Because these two types of solute diffuse at very different rates, there are difficulties in using the theory for diffusion controlled growth with local equilibrium at the interface, as applied to binary alloys. In particular, it is necessary to ensure mass balance for all species at the moving interface in spite of their different diffusivities. There is published work which has dealt consistently with the multicomponent nature of the precipitation process,[1,2] but those models did not account for the consumption of nucleation sites as precipitation proceeds. As a consequence, the number density of precipitates could exceed the number density of nucleation sites.

In previous work,[5] the precipitation of molybdenum carbide needles in ferrite was modelled, taking proper account of the diffusion of molybdenum and carbon, together with capillarity effects. The fact that molybdenum carbide precipitation in ferrite is preceded by that of cementite was also taken into account. By contrast, niobium carbide precipitates directly from austenite making the development of a kinetic model comparatively simple. Furthermore, its shape approximates that of a sphere, which is easier to deal with in the context of coarsening. The purpose of the present work was to develop an overall transformation kinetics model for the precipitation of niobium carbides in austenite, including multicomponent diffusion and capillarity in such a way as to allow the precipitation and coarsening process to be treated in a unified scheme.

Method

The maximum volume fraction of the niobium carbide is very small, typically 0·001, so the probability of impingement between particles nucleated at different locations is similarly small. It can reasonably be assumed that each particle, once nucleated, can grow freely. Its size can therefore be monitored as transformation proceeds. Indeed, the size of all particles that form can be followed for any instant of time, as can the mean particle spacing which is a function of the instantaneous number density of carbides. To do this requires nucleation and growth functions, which are well established and hence are presented briefly in the discussion that follows.

Nucleation

Following Turnbull and Fisher,[6] the nucleation rate per unit volume is given by

$$I = \bar{c}\left(1-\frac{V^{\omega}}{V^{\omega\gamma}}\right) N_0 \frac{kT}{h} \exp\left(-\frac{G^*+Q}{kT}\right) \quad . \; . \; . \quad (1)$$

where $\bar{c}$ is the concentration of the most slow moving solute (in this case niobium), G^* is the activation energy for nucleation, Q is the activation energy for diffusion, k and h are the Boltzmann and Planck constants respectively, T is temperature, N_0 is the initial number density of nucleation sites, V^{ω} is the volume fraction of niobium carbide (ω), and $V^{\omega\gamma}$ the volume fraction of niobium carbide which is in equilibrium with austenite (γ). The term $(1-V^{\omega}/V^{\omega\gamma})$ has been incorporated into the classical equation to account for the fact that nucleation sites are consumed as transformation proceeds. This term has been neglected in previous analyses where it is easy to show that the number density of precipitates soon exceeds N_0, a situation which is unphysical and misleading in the context of coarsening reactions. Note that the term $(1-V^{\omega}/V^{\omega\gamma})$ is commonly used in Avrami theory to account for matrix which can no longer contribute to transformation.[7]

The activation energy G^* for a spherical nucleus is given by

$$G^* = \frac{16\pi\sigma^3}{3(\Delta G_{\mathrm{V}})^2} \quad . \; . \; . \; . \; . \; . \; . \; . \; . \; . \; . \; . \quad (2)$$

where σ is the niobium carbide/austenite interfacial energy per unit area, ΔG_{V} is the chemical free energy change per unit volume of precipitate. The precipitation reaction is

$$\gamma \rightarrow \gamma' + \omega \quad . \; . \; . \; . \; . \; . \; . \; . \; . \; . \; . \; . \; . \quad (3)$$

where γ' represents the austenite which is in equilibrium with niobium carbide. The free energy change for this reaction ΔG_0, calculated using MTDATA[8] with the SGTE

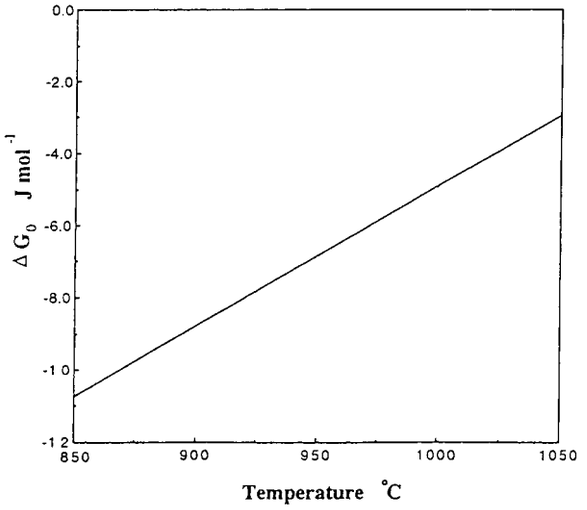

1 Free energy change ΔG_0 as function of temperature for Fe–0·1C–0·05Nb (wt-%) steel, calculated using MTDATA[8]

database, is shown in Fig. 1. The free energy change ΔG_V is given by

$$\Delta G_V = \frac{\Delta G_0}{V^{\omega\gamma} V_M^{\omega}} \quad \ldots\ldots\ldots\ldots\ldots\ldots \quad (4)$$

where V_M^{ω} is the molar volume of niobium carbide.

Growth

A reasonable approximation for isothermal diffusion controlled growth is that the compositions of the phases in contact at the interface are locally in equilibrium. It follows that for a binary alloy these compositions are given by a tie-line of the equilibrium phase diagram; for a binary system, the tie-line is unique and passes through $\bar{c}$ which is the average concentration of solute in the alloy. The concentration profile which develops during the precipitation of a solute rich phase, such as a carbide, from a matrix is shown schematically in Fig. 2, where $c^{\gamma\omega}$ is the concentration of solute in austenite which is in equilibrium with niobium carbide and $c^{\omega\gamma}$ is the concentration of solute in niobium carbide which is in equilibrium with austenite. For local equilibrium to be maintained, the rate at which solute is partitioned into the carbide must equal the rate at which it arrives at the interface by diffusion, giving the conservation condition

$$v(c^{\omega\gamma} - c^{\gamma\omega}) = -D \left.\frac{\partial c}{\partial z}\right|_{z=z^*} \quad \ldots\ldots\ldots\ldots \quad (5)$$

where v is the velocity of interface, z is a coordinate normal to the interface, z^* is the position of the interface on the coordinate z, and D is the diffusion coefficient of the solute in austenite. The concentration gradient is evaluated at the position of the interface, $z=z^*$.

For a ternary alloy, the tieline will not in general pass through $\bar{c}$ because it is necessary to simultaneously satisfy two conservation equations at the interface, one each for niobium and carbon which diffuse at very different rates

$$\left.\begin{aligned} v(c_{Nb}^{\omega\gamma} - c_{Nb}^{\gamma\omega}) &= -D_{Nb} \left.\frac{\partial c_{Nb}}{\partial z}\right|_{z=z^*} \\ v(c_C^{\omega\gamma} - c_C^{\gamma\omega}) &= -D_C \left.\frac{\partial c_C}{\partial z}\right|_{z=z^*} \end{aligned}\right\} \quad \ldots\ldots\ldots \quad (6)$$

However, according to the phase rule there is an additional degree of freedom in a ternary alloy so there are many

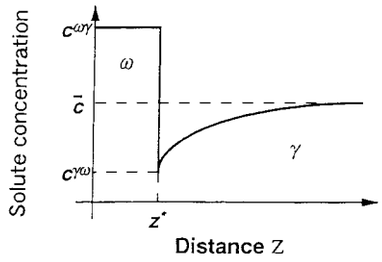

2 Schematic diagram of solute concentration profile during diffusion controlled precipitation of NbC (ω) from austenite (γ): $\bar{c}$ is average concentration of solute in alloy, $c^{\gamma\omega}$ is concentration of solute in γ which is in equilibrium with ω, $c^{\omega\gamma}$ is concentration of solute in ω which is in equilibrium with γ, and z^* is position of interface on coordinate normal to interface

tielines defining $\omega-\gamma$ equilibrium, available at any given temperature. It is then possible to select a tieline from the two phase $\omega+\gamma$ field which is able to satisfy both of these equations in spite of the fact that $D_C \gg D_{Nb}$, while at the same time maintaining local equilibrium.[9,10]

There are two ways in which this can happen.[9,10] The first is for the system to choose a tieline which greatly increases the gradient of niobium to compensate for its low diffusivity. This would require the carbide to have virtually the same niobium concentration as the matrix with very little partitioning of niobium, but with a sharp concentration spike at the interface in order to maintain local equilibrium. This is only possible at very large driving forces and hence is not applicable to niobium carbide precipitation in microalloyed steels. The more relevant alternative is to select a tieline which reduces the gradient of carbon to such an extent that the flux of carbon is reduced to a level consistent with that of niobium.

Referring to Fig. 3, the intersection of the vertical line with the $\gamma/(\gamma+\omega)$ phase field defines completely the tieline which fixes the interface compositions in a manner which satisfies the conservation conditions because the large diffusion coefficient of carbon is compensated for by the very small concentration gradient of carbon.[9,10]

All this assumes that the far field concentration $\bar{c}$ does not change during transformation, i.e. there is no 'soft impingement' of the diffusion fields of different particles. However, soft impingement is inevitable for the later stages of transformation, in which case the tieline controlling interface compositions must change to continue to satisfy the conservation conditions. The locus of the matrix

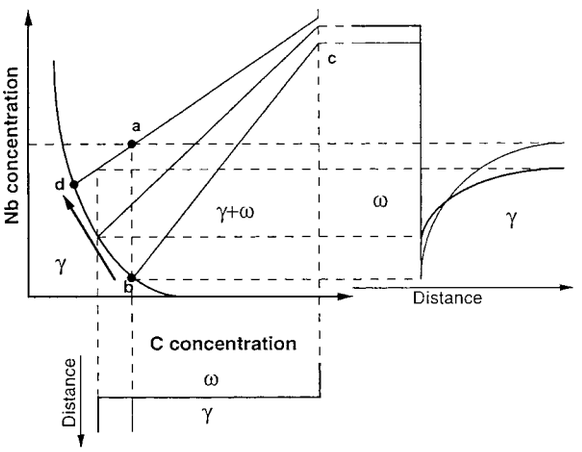

3 Schematic diagram of isothermal section through Fe–C–Nb phase diagram, showing γ and ω phase fields: average composition of alloy is plotted as point a

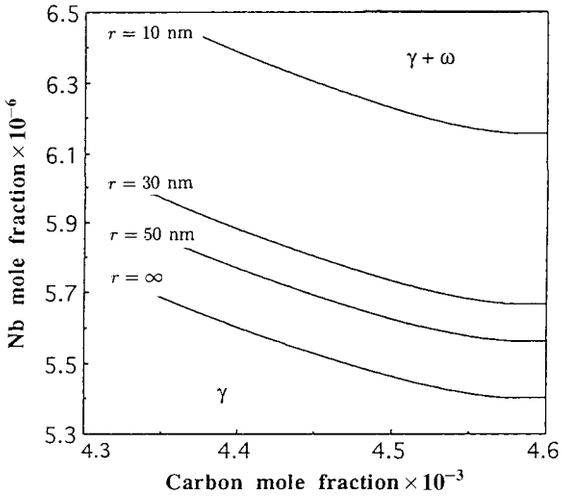

4 $\gamma/\gamma+\omega$ phase boundaries in isothermal section of Fe–C–Nb phase diagram at 900°C with illustration of influence of capillarity: $\sigma=0{\cdot}25$ J m^{-2}

composition due to solute depletion during precipitation is along the direction a → d (Fig. 3). The change in the matrix composition also leads to a different choice of tieline, the locus of $c^{\gamma\omega}$ being along b → d (Fig. 3). This tieline shifting continues until the reaction stops when the tieline intersects the average composition a and $c^{\gamma\omega}=$ d.

The mean field approximation is used to calculate changes in $\bar{c}$ as precipitation proceeds. The instantaneous value of the matrix compositions, $\bar{c}'$, is given by

$$\bar{c}'=\bar{c}-\frac{V^{\omega}(c^{\omega\gamma}-\bar{c})}{1-V^{\omega}} \quad \ldots\ldots\ldots\ldots \quad (7)$$

Once the interface compositions are defined as described above, established theory for diffusion controlled growth can be applied to estimate the particle radius r as a function of time[7] t

$$r=\alpha_3(Dt)^{1/2} \quad \text{with} \quad \alpha_3\approx\left(2\,\frac{\bar{c}-c^{\gamma\omega}}{c^{\omega\gamma}-\bar{c}}\right)^{1/2} \quad \ldots\ldots \quad (8)$$

where α_3 is the three-dimensional parabolic rate constant.

The driving force for nucleation must also be affected by the effect of soft impingement. To deal with this, an extent of reaction parameter is defined as follows

$$\Phi=\frac{V^{\omega}}{V^{\omega\gamma}} \quad \text{with} \quad V^{\omega\gamma}=\frac{\bar{c}-c^{\gamma\omega}}{c^{\omega\gamma}-c^{\gamma\omega}} \quad \ldots\ldots\ldots \quad (9)$$

where V^{ω} is the instantaneous fraction and $V^{\omega\gamma}$ the maximum fraction of a given phase. The function Φ ranges from 0 to 1 and represents the fraction of excess solute remaining in the matrix relative to the equilibrium composition of the precipitate. It is assumed that the driving force for precipitation (equation (4)) is related linearly to Φ

$$\Delta G=(1-\Phi)\Delta G_0 \quad \ldots\ldots\ldots\ldots\ldots \quad (10)$$

where ΔG_0 is described in equation (4).

Capillarity

The state of equilibrium between two phases changes with the curvature of the interface separating them according to the well established capillarity effect, which scales with the interfacial energy;[7] the capillarity effect is often also called the Gibbs–Thompson effect. The free energy of a carbide phase varies relatively sharply with deviations from the stoichiometric composition so it can be assumed that the carbide composition is insensitive to the curvature. However, the equilibrium composition of the matrix changes as follows[7]

$$c_{\mathrm{r}}^{\gamma\omega}=\left(1+\frac{\sigma}{kT}\,\frac{2V_{\mathrm{M}}^{\omega}}{r}\,\frac{1-c^{\gamma\omega}}{c^{\omega\gamma}-c^{\gamma\omega}}\right)c^{\gamma\omega} \quad \ldots\ldots \quad (11)$$

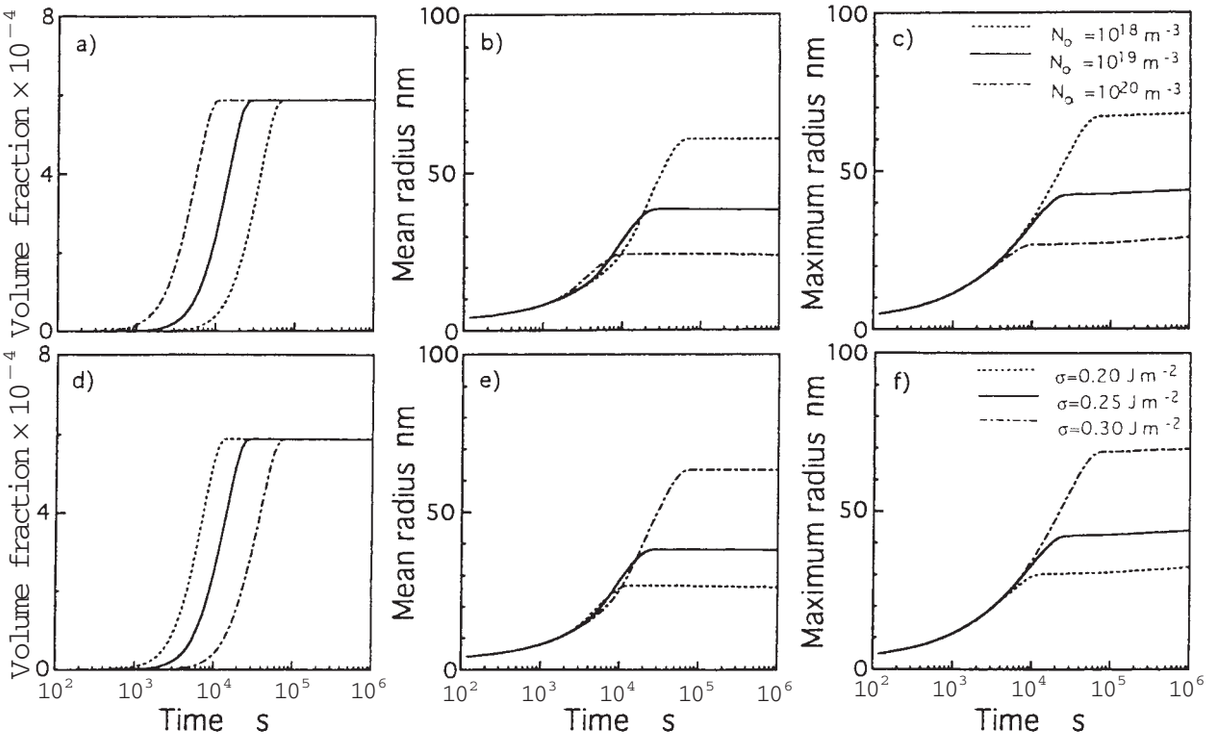

5 Effect of *a–c* number density of nucleation sites N_0 ($\sigma=0{\cdot}25$ J m^{-2}) and *d–f* interfacial energy σ ($N_0=10^{19}$ m^{-3}) on volume fraction and sizes of NbC precipitates in austenite: equilibrium fraction of NbC at 900°C is 0·00059

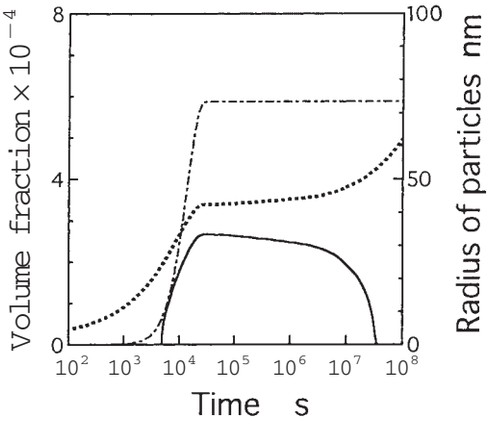

6 Calculated data on volume fraction (·····) and radius changes for large (····) and small (—) particles of NbC at 900°C with $N_0 = 10^{19}$ m^{-3} and $\sigma = 0{\cdot}25$ J m^{-2}

where $c_r^{\gamma\omega}$ is the solute concentration in austenite which is in equilibrium with a spherical particle of niobium carbide and r is the radius of curvature (which in this case also defines the particle size): $c^{\gamma\omega} = c_r^{\gamma\omega}$ when $r = \infty$. The modified composition $c_r^{\gamma\omega}$ is therefore easy to estimate for each particle.

For a ternary alloy, capillarity is dealt with by calculating the $\gamma/\gamma + \omega$ phase boundary on an isothermal section of the phase diagram, as a function of r using equation (11). The growth velocity can then be calculated using the curvature modified phase boundary.[5] Figure 4 shows an example of the modified isothermal section of the phase boundaries between niobium carbide and austenite.

Particles that are smaller than the size of a critical nucleus obviously cannot grow. Nucleation occurs by random fluctuations so that the growth part in the computational scheme must start beyond the nucleation stage. Particles nucleate at different times during the course of reaction, giving thereby a distribution of sizes. At any given stage of precipitation, the small particles will grow at a slower rate than larger particles because the capillarity effect reduces the supersaturation for small particles. The condition that particles which have nucleated can grow is given by

$$(\bar{c}' - c_r^{\gamma\omega}) > 0 \quad \ldots\ldots\ldots\ldots\ldots\ldots \quad (12)$$

Capillarity has the consequence that large particles have higher solute concentrations at the interface $c_r^{\gamma\omega}$ than small particles. This drives coarsening which becomes a natural consequence of the precipitation theory since changes, including the dissolution of particles, continue to happen as long as there are solute concentration gradients.

Some calculations

Calculations were carried out for a Fe–0·1C–0·05Nb (wt-%) steel, a typical composition for a high strength low alloy steel. The following values of D_0 in the diffusion coefficient and of activation energy for diffusion of niobium in austenite were used:[11] $0{\cdot}56 \times 10^{-4}$ m^2 s^{-1} and 286×10^3 J mol^{-1}, respectively.

There are two unknown parameters, the number density of nucleation sites N_0 and the interfacial energy σ. Figure 5 shows calculated changes in the volume fraction and in the mean and maximum particle radius with N_0 and σ for precipitation at 900°C. As expected, smaller values of N_0 reduce the overall rate of reaction but lead to larger particle radii. A smaller interfacial energy facilitates the reactions so that equilibrium is achieved earlier.

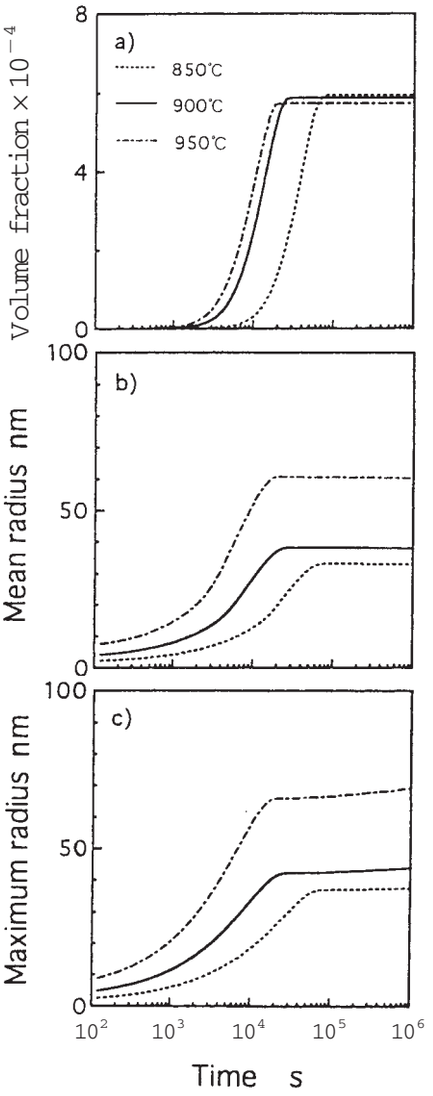

7 Volume fraction and particle radii for NbC at 850, 900, and 950°C with $N_0 = 10^{19}$ m^{-3} and $\sigma = 0{\cdot}25$ J m^{-2} as function of time: equilibrium fractions of NbC at 850, 900, and 950°C are 0·00059, 0·00059, and 0·00058 respectively

Although Okamoto and Suehiro[2] change the interfacial energy σ as particles grow, Miyazaki[12] has shown that a single value of σ can describe the entire range of particle sizes. Therefore, in this work, σ was assumed to be constant during precipitation. Figure 6 shows how the particle radius and volume fraction change with time at 900°C using reasonable values of $N_0 = 10^{19}$ m^{-3} and $\sigma = 0{\cdot}25$ J m^{-2}. The large particle, which nucleated in the early stages of precipitation, grows continuously even as the volume fraction approaches equilibrium. However, because of the capillarity effect, the small particle which nucleated in the later stages begins to dissolve even though the large particle continues to grow. Similar data for 850, 900, and 950°C are shown in Fig. 7.

Manganese and silicon are common alloying elements in steels. Their thermodynamic effect on niobium carbide precipitation is shown in Fig. 8. Neither element has a large effect on the driving force for niobium carbide formation. Figure 9 shows the changes in volume fraction and particle sizes at 900°C with $N_0 = 10^{19}$ m^{-3} and $\sigma = 0{\cdot}25$ J m^{-2} for Fe–0·1C–0·05Nb and Fe–0·1C–1Si–0·05Nb (all wt-%) steels. There are only minor differences which may be neglected for all practical purposes.

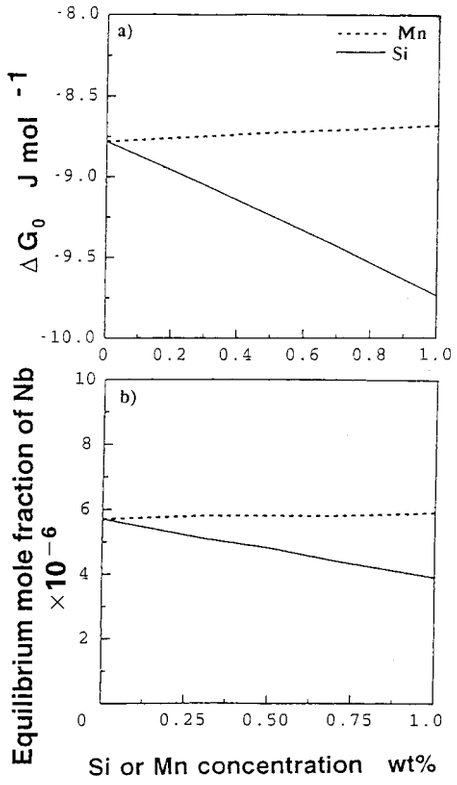

8 Effect of Mn and Si *a* on free energy change ΔG_0 for precipitation of NbC from austenite and *b* on equilibrium mole fraction of Nb in matrix for Fe–0·1C–0·05Nb (wt-%) steel at 900°C

Coarsening

Figure 10 shows the calculated changes in the mean radius and number density of niobium carbide at 900°C for Fe–0·1C–0·05Nb steel. This general behaviour has also been reported for a Cu–Ti alloy[13] and a microalloyed steel.[2] As expected, the radius at first changes parabolically with time, corresponding to the stage where precipitation is the dominant process. There is then a flat 'stasis' region where little seems to happen. This is followed by the onset of coarsening[14] where the mean particle radius tends to change in proportion to $t^{1/3}$. This is known as Ostwald ripening.

In the stasis region, some particles are beginning to dissolve, as is also evident from the plots shown in Fig. 6. However, most of the particles nucleate at an early stage of transformation (Fig. 10*b*) so it takes considerable time for the smaller among them to dissolve, given that this coarsening phenomenon is driven by very small capillarity induced concentration gradients.

One computational problem with calculations of this kind is that the time scales associated with the precipitation and with the coarsening stages are very large. Caution must therefore be exercised to avoid the accumulation of numerical errors. The computational time steps were chosen to avoid these difficulties without making the calculation time intolerable.

Comparison with experimental data

Although there are many data about the precipitation of niobium carbide during the hot deformation of austenite in microalloyed steels, similar data for isothermal heat treatment are difficult to find. Akamatsu *et al.*[1] investigated niobium carbide precipitation in niobium added microalloyed steels. From their observations using transmission electron microscopy of samples isothermally heat treated at 900°C in a Fe–0·11C–0·26Si–1·1Mn–0·045Nb (wt-%) steel, they were able to estimate the niobium carbide particle size as a function of time. These data are available for the early stages of precipitation rather than coarsening. Calculations were done using an interfacial energy $\sigma = 0{\cdot}26$ J m^{-2} and a fitted number density of nucleation sites $N_0 = 9 \times 10^{19}$ m^{-3} as shown in Fig. 11. The particle size has error bars which correspond to two standard deviations. There is reasonable agreement between theory and experiments. However, the experimental data are rather limited in quantity so more experiments would clearly be useful.

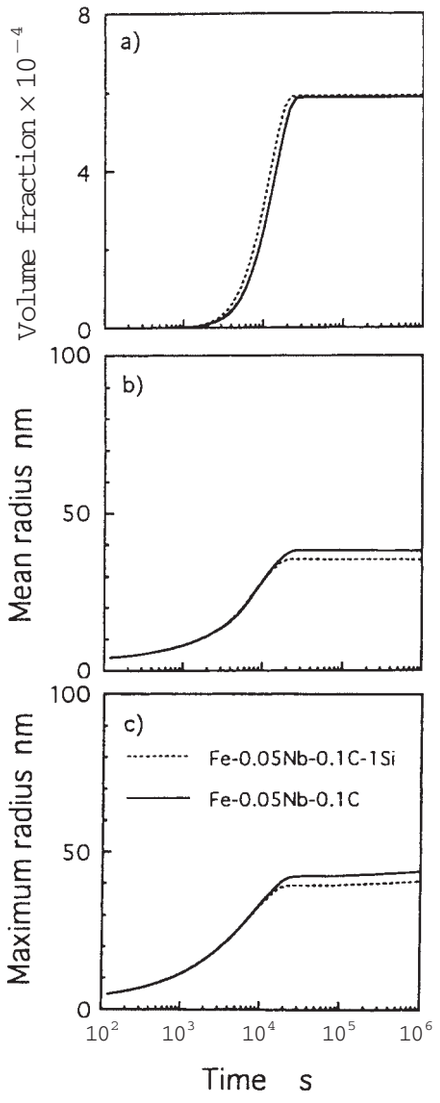

9 Particle radii and volume fractions as function of time at 900°C in Fe–0·1C–0·05Nb and Fe–0·1C–1Si–0·05Nb (all wt-%) steels

Summary

A methodology has been developed to deal with the growth of spherical precipitates, in this case, niobium carbide in a

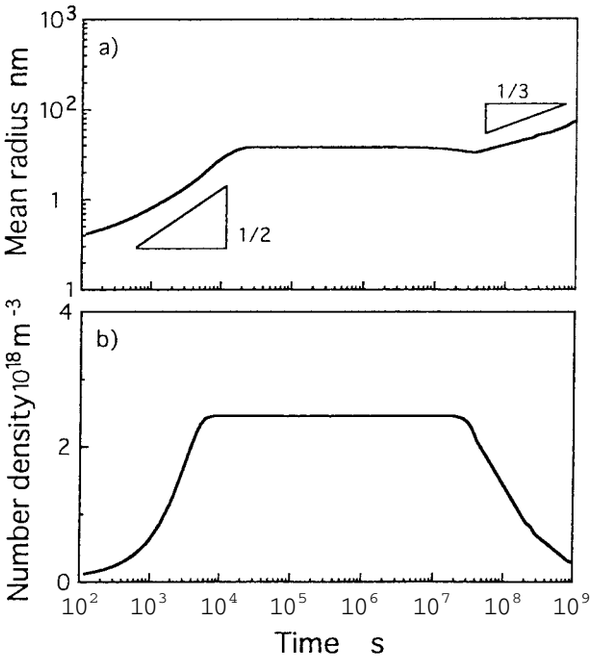

10 *a* particle radius and *b* number density of NbC precipitates as function of time at 900°C in Fe–0·1C–0·05Nb steel with $N_0 = 9 \times 10^{19}$ m^{-3} and $\sigma = 0{\cdot}26$ J m^{-2}

ternary alloy, properly taking into account mass balance during diffusion controlled growth while at the same time dealing with capillarity effects and nucleation site consumption. The model has been able to simulate the entire precipitation process including coarsening. There is reasonable agreement with the rather limited experimental data that are available.

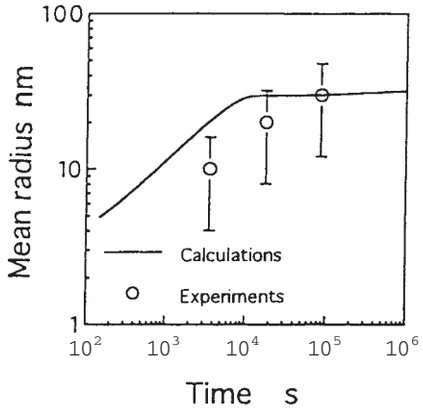

11 Comparison between calculations ($N_0 = 9 \times 10^{19}$ m^{-3} and $\sigma = 0{\cdot}26$ J m^{-2}) and experimental data (Akamatsu *et al.*[1]) for NbC particle growth with holding time at 900°C in Fe–0·11C–0·26Si–1·1Mn–0·045Nb (wt-%) steel

Acknowledgement

The authors are grateful to Nippon Steel Corporation for funding this research and to Professor A. Windle for the provision of laboratory facilities at the University of Cambridge. One of the authors (NF) would like to express thanks to R. Okamoto, Dr M. Takahashi, H. Suehiro, and S. Akamatsu for useful discussions.

References

1. S. AKAMATSU, Y. MATSUMURA, T. SENUMA, H. YADA, and S. ISHIKAWA: *Tetsu-to-Hagane (J. Iron Steel Inst. Jpn)*, 1989, **75**, 933–940.
2. R. OKAMOTO and M. SUEHIRO: *Tetsu-to-Hagane (J. Iron Steel Inst. Jpn)*, 1998, **84**, 650–657.
3. A. LE BON, J. ROFES-VERNIS, and C. ROSSARD: *J. Met. Sci.*, 1975, **9**, 36–40.
4. B. DUTTA and C. M. SELLARS: *Mater. Sci. Technol.*, 1987, **3**, 197–206.
5. N. FUJITA and H. K. D. H. BHADESHIA: *Mater. Sci. Technol.*, 1999, **15**, 627–634.
6. D. TURNBULL and J. C. FISHER: *J. Chem. Phys.*, 1949, **17**, 71–73.
7. J. W. CHRISTIAN: 'Theory of transformations in metals and alloys', 2 edn, Part 1; 1975, Oxford, Pergamon.
8. D. E. COATES: *Metall. Trans.*, 1973, **4**, 2313–2325.
9. J. S. KIRKALDY: *Can. J. Phys.*, 1958, **36**, 907–916.
10. S. M. HODSON: 'MTDATA – Metallurgical and thermochemical databank'; 1989, Teddington, National Physical Laboratory.
11. Metals Data Book, 1993, Tokyo, The Japan Institute of Metals.
12. T. MIYAZAKI: in 'Solid–solid phase transformations '99', (ed. M. Koiwa *et al.*), 15–22; 1999, Tokyo, The Japan Institute of Metals.
13. R. WAGNER and R. KAMPMANN: in 'Materials science and technology', (ed. R. W. Cahn *et al.*), Vol. 5, 272–293; 1991, New York, VCH.
14. I. M. LIFSHITZ and V. V. SLYOZOV: *J. Phys. Chem. Solid.*, 1961, **19**, 35–50.